

## ASPECTS OF SPECIFIC DNA-PROTEIN INTERACTION; LOCAL BENDING OF DNA MOLECULES BY IN-REGISTER BINDING OF THE OLIGOPEPTIDE ANTIBIOTIC DISTAMYCIN

Karl Ernst REINERT

*Academy of Sciences of the GDR, Central Institute of Microbiology and Experimental Therapy  
Department of Biophysical Chemistry, DDR-69 Jena, GDR*

Received 18 April 1980

Distamycin A binds strongly/moderately to DNA below/above  $r = 0.08$  molecules bound per DNA phosphate. Titration viscometric measurements for high and low molecular weight DNA yielded the relative changes of DNA persistence length,  $\Delta a/a^0$ , and contour length,  $\Delta L/L^0$  (Nucl. Acids Res. 7 (1979) 1375).  $\Delta L/L^0$  is negligible/positive in the range below/above  $r = 0.08$  at 0.2 M Na<sup>+</sup>. A two-line covering of the small groove by ligand molecules explains the increase of contour length. The characteristic  $\Delta a/a^0$  drop is quantitatively interpreted by local DNA bending (kinking). The underlying theoretical basis is presented in two appendices and applied, in a third one, to literature data for the DNA-actinomycin system.

The angle  $\gamma$  of local DNA bending as induced by complex formation with different distamycin derivatives is presented for DNA species of different base composition. By means of an appropriate model, a length mismatch per dinucleotide of  $(0.032 \pm 0.01)$  nm [or  $(0.043 \pm 0.01)$  nm] was derived from the experimentally obtained bending angle per dinucleotide of  $(1.6 \pm 0.4)^\circ$  [or  $(2.1 \pm 0.05)^\circ$ ], independent of DNA base composition and distamycin chain length.

### 1. Introduction

Recognition between nucleic acids and protein molecules at repression, initiation and termination of nucleic acid synthesis involves the formation of hydrogen bonds between specifically interacting groups of both components. Different models have been developed to explain specificity and code (see, e.g., [1–5]). Nevertheless, we are far from understanding all details. That is why the derivation of data, quantitatively describing the interaction of DNA with specifically binding compounds, is a suitable approach to this problem. Appropriate oligopeptides are the antibiotics netropsin and distamycin<sup>‡</sup>. Both effectors inhibit the DNA template activity *in vitro* [6–8]. These oligopeptides preferentially interact with (A·T)-rich DNA sequences in the small groove, obviously by in-register binding of the components [9–14]. They are able to form structures being *nearly* isogeometrical complements to B-form DNA [15,16].

The different hydrodynamic behaviour of DNA

upon interaction with the compounds mentioned [17–19] indicates different local DNA conformational changes. For DNA-netropsin interaction several distinct, mainly sequence dependent modes could be distinguished. They were characterized by the degree of local DNA-stiffening and, for the three modes of strongest interaction, by a characteristic species-independent elongation of the helix [14]. For Dst interaction with DNA at physiological salt concentration it has qualitatively been pointed out recently that this oligopeptide induces a local DNA-bending, but without a significant elongation at low degree of binding [19], contrary to the same system investigated at 0.0025 M Na<sup>+</sup> by electric dichroism [20].

It is a main subject of this paper to analyse quantitatively the interaction mechanism at 0.2 M Na<sup>+</sup> for this recognition model. By means of theoretical considerations described in the appendices A and B the bending angle  $\gamma$  was derived. Basing on this result the length difference in the binding pattern of the two components, DNA and Dst, was estimated. The formalism presented enables us to analyse viscosity data formerly obtained with DNA of different base composition and with Dst derivatives of different chain length [19]. These findings demonstrate, for a special

<sup>‡</sup> *Abbreviations.* Dst: distamycin, Dst-*n*: Dst with *n* methylpyrrole rings (*n* = 3, 4, 5), Dst-3  $\equiv$  distamycin A, Dst-D: desformyl-Dst-3; Acm: actinomycin.

example, the possibility to fix a DNA helix curvature by in-register constraints of peptidic ligands and double helix. The competence of the theoretical background is illustrated in appendix C by means of an analysis of literature data for the system DNA-actinomycin. Some biological implications are discussed.

## 2. Materials and methods

### 2.1. Materials

*Distamycin A* with its three methylpyrrolicarboxamide units (Dst-3) was a gift of Drs. Ch. Zimmer and F. Arcamone. Its chemical structure is shown in fig. 1. *Calf thymus DNA* was isolated by Dipl. Chem. Eva Sarfert [21], Department of Biochemistry. A low (*l*) and a high (*h*) molecular weight DNA sample were used. (*l*: sonication at 3°C in an inert gas atmosphere; *h*: sheared by means of a syringe to get a molecular weight sufficiently low to prevent an influence of the "excluded volume effect" [22,23]. Solvent: 0.15 M NaCl plus 0.015 M sodium citrate; residual protein content: 0.15%.

### 2.2. Viscometry

The titration technique applied in rotational viscometry was described elsewhere [14]. It permits to reduce the error in the *change* of viscosity by at least one order of magnitude. The relative change of intrinsic viscosity,  $\Delta\eta = \Delta[\eta]/[\eta]^0$ , was approximated by  $\Delta(\ln \eta_{\text{rel}}/c)/(\ln \eta_{\text{rel}}^0/c^0)$  [24,25]. The error in  $\Delta\eta$  resulting from this assumption can be shown to be negligible, in particular owing to the fairly low values of  $(\eta_{\text{rel}}-1)$ .

### 2.3. Binding data

The *binding isotherm* was approximated by means of a model-free analysis. The underlying ideas were first published in detail by Revet et al [25a] and Halfman and Nishida [26] (cf. also [18,27–29]).

*Per definitionem*,  $r_t = c_{\text{Dst}}^{\text{total}}/c_P = (c_{\text{Dst}}^{\text{bound}} + c_{\text{Dst}}^{\text{free}})/c_P$  ( $c_P$  is the DNA phosphate concentration;  $c_{\text{Dst}}^{\text{total}}$ ,  $c_{\text{Dst}}^{\text{bound}}$ ,  $c_{\text{Dst}}^{\text{free}}$  the molar concentrations of total, bound and unbound Dst, respectively;  $r = c_{\text{Dst}}^{\text{bound}}/c_P$ ). For very strong binding,  $c_{\text{Dst}}^{\text{free}} \ll c_{\text{Dst}}^{\text{bound}}$  and, consequent-

ly,  $r_t \approx r$  independent of the polymer concentration  $c_P$ . Weaker binding means:  $c_{\text{Dst}}^{\text{free}}$  is comparable with  $c_{\text{Dst}}^{\text{bound}}$ . For two Dst-DNA solutions of the same  $r$  but different  $c_P$  value  $c_{\text{Dst}}^{\text{free}}$  must be the same.  $c_{\text{Dst}}^{\text{free}}/c_P$ , however, now depends on  $c_P$  and, consequently, it is  $r_t > r$ . The difference between  $r_t$  and  $r$  decreases with increasing  $c_P$  and vanishes at  $c_P \rightarrow \infty$ . With the criterion "equal magnitude of  $\Delta y$  means equal value of  $r$ " it follows

$$r = \Delta c_{\text{Dst}}^{\text{total}}/\Delta c_P, \quad c_{\text{Dst}}^{\text{free}} = \Delta r_t/\Delta(1/c_P) \quad (1a, b)$$

independent of whether the binding is co-operative or not but provided that no disturbing polymer–polymer association exists. ( $\Delta y$  was approximated as mentioned above. Generally,  $\Delta y$  may be any suitable physical, chemical, or even biological *intensive* [22] quantity.) The differences  $\Delta c_{\text{Dst}}^{\text{total}}$ ,  $\Delta c_P$ ,  $\Delta r_t$  and  $\Delta(1/c_P)$  have to be taken from the  $\Delta y$  versus  $r_t$  curves for different  $c_P$  values at, in each case, equal  $\Delta y$ .

An apparent mean *association constant*  $K_{\text{app}}$  can roughly be estimated [22] from the half-saturation concentration  $^{50\%}c_{\text{Dst}}^{\text{free}}$  according to

$$K_{\text{app}} = 1/(^{50\%}c_{\text{Dst}}^{\text{free}}). \quad (1c)$$

### 2.4. Conformational changes

The relative *change of DNA persistence length*,  $\Delta a/a^0$ , and contour length,  $\Delta L/L^0$ , for the almost coil-like and more rod-like DNA molecules investigated (with  $M_h = 12.5 \times 10^6$  and  $M_l = 0.55 \times 10^6$ , respectively) were obtained as the solutions of the following two equations

$$\begin{aligned} \Delta y_h = & 1.195 (\Delta a/a^0) + 1.735 (\Delta L/L^0) \\ & + 0.06 (\Delta a/a^0)^2 + 0.63 (\Delta L/L^0)^2 \\ & + 2.18 (\Delta a/a^0) (\Delta L/L^0), \end{aligned} \quad (2a)$$

$$\begin{aligned} \Delta y_l = & 0.585 (\Delta a/a^0) + 2.22 (\Delta L/L^0) \\ & - 0.28 (\Delta a/a^0)^2 + 1.18 (\Delta L/L^0)^2 \\ & + 1.60 (\Delta a/a^0) (\Delta L/L^0). \end{aligned} \quad (2b)$$

$\Delta y_h$  and  $\Delta y_l$  are the  $\Delta y$  values, measured as a function of  $r$ , for the two DNA samples (fig. 1). The coefficients for the first and second order approximation

were taken from paper [23]. (See also fig. 1 of [14] for an illustrative demonstration of the problem.) It is assumed that the worm-like coil concept is a reasonable approximation also for short locally bent DNA molecules (cf. [30]). The hydrodynamically equivalent helix diameter  $b^0$  of DNA amounts to approximately 3.0 nm [31,32]. We can assume  $\Delta b/b^0 \approx 0$  [18,23] for binding of small linear ligands inside the narrow groove.

For high molecular weight coil-like DNA molecules with negligible influence of the excluded volume [22, 23] and vanishing  $\Delta L/L^0$  the first order approximation

$$\Delta y_h = K_a (\Delta a/a^0) \quad (2c)$$

describes the  $\Delta a/a^0$  versus  $r$  dependence. This follows from the small values of the coefficient for the  $(\Delta a/a^0)^2$  term in the second order approximation (cf. eq. (2a)). The values of  $K_a$  for the different DNA samples were taken from paper [23] and are listed in table 1.

The criteria for ligand binding induced local bending or kinking and an equation for the determination of the bending angle  $\gamma$  from the relative change of persistence length are presented in the appendices A and B.

The change of DNA contour length per bound ligand molecule is given by the relation

$$\Delta L_{1Dst} = \frac{0.34 \text{ nm}}{2} \frac{d}{dr} (\Delta L/L^0). \quad (3)$$

The influence of polydispersity upon the results of this paper has to be assumed to be effectively very low [14].

### 3. Results and discussion

#### 3.1. Viscosity of Dst-3 complexes with calf thymus DNA; binding properties

In fig. 1 the relative change of the intrinsic viscosity

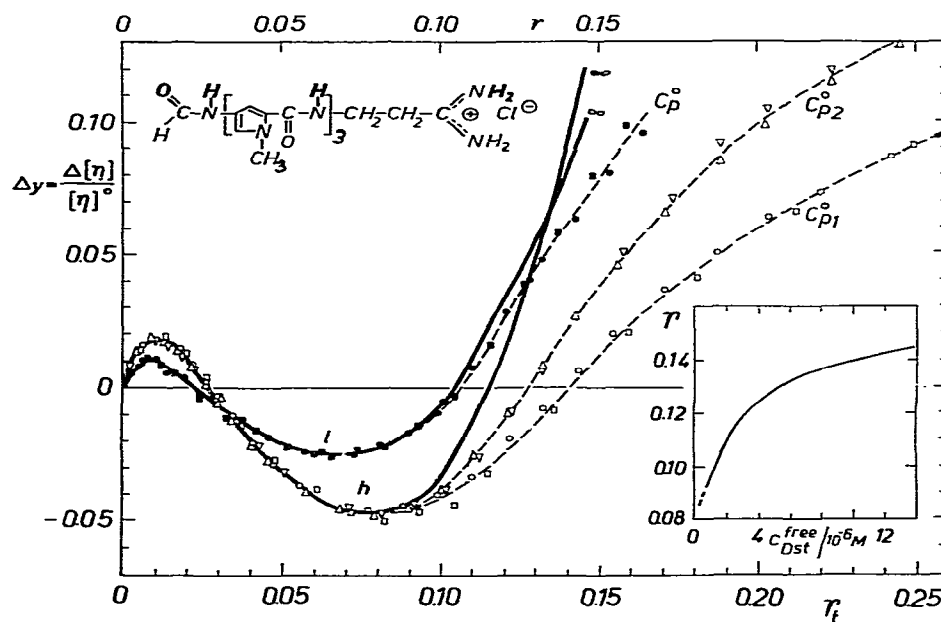


Fig. 1. Relative change of calf thymus DNA viscosity,  $\Delta y = \Delta[\eta]/[\eta]^0$ , as a function of the molar concentration ratio of added Dst-3 and DNA phosphate ( $r_t$ ; ---), and as a function of the concentration ratio of bound Dst-3 and DNA phosphate ( $r$ ; —) ( $0.2 \text{ M Na}^+$ ,  $20^\circ\text{C}$ ,  $\text{pH } 7$ );  $M_h = 12.5 \times 10^6$  ( $c_{P1}^0 = 1.05 \times 10^{-4} \text{ M}$  DNA-phosphate,  $\eta_{rel,1}^0 = 1.252$ ;  $c_{P2}^0 = 2.15 \times 10^{-4} \text{ M}$ ,  $\eta_{rel,2}^0 = 1.580$ ),  $M_l = 0.55 \times 10^6$  ( $c_P^0 = 9.78 \times 10^{-4} \text{ M}$ ,  $\eta_{rel}^0 = 1.150$ ), ( $c_P^0$  and  $\eta_{rel}^0$ : concentration and relative viscosity, respectively, of the solution of DNA before ligand addition). Insert: Binding isotherm derived from the two  $\Delta y$  versus  $r_t$  curves for the high molecular weight DNA sample as described in section 2.3.

for calf thymus DNA at 0.2 M Na<sup>+</sup> and 20°C is plotted as a function of the concentration ratio of *added* Dst-3 molecules per DNA phosphate ( $r_t$ ; lower scale) and as a function of the ratio of *bound* ligand molecules per DNA-P ( $r$ ; upper scale). In order to get a quantitative analysis of DNA conformational changes the measurements had to be performed for both almost coil-like (*h*) and more rod-like (*l*) DNA molecules.

The (approximated) binding isotherm (insert of fig. 1) was derived from the experimental viscometric "titration curves"  $\Delta y$  versus  $r_t$ , measured at different DNA concentrations  $c_p^0$ , as explained in section 2.3. With these data we were able to construct the  $\Delta y$  versus  $r$  plots. At  $r_t < 0.08$  the coincidence of the  $\Delta y$  versus  $r_t$  curves for the different  $c_p^0$  values indicates that  $c_{Dst}^{free} \ll c_{Dst}^{bound}$  and, in good approximation,  $r_t = r$ . By means of eqs. (1b,c) we estimate 50%  $c_{Dst}^{free} < 2 \times 10^{-7}$  M and, consequently,  $K_{app} > 5 \times 10^6$  M<sup>-1</sup>. Dialysis experiments in the same solvent [33] yielded  $K = 2.4 \times 10^9$  M<sup>-1</sup> [34] and confirm this consideration. Above  $r_t = 0.08$  the divergence of the  $\Delta y$  versus  $r_t$  curves indicates that the concentration of free and bound Dst are now comparable. The  $K_{app}$  value for this range can be estimated from eq. (1c) at approximately  $3 \times 10^5$  M<sup>-1</sup> in good accord with other independent results [34]. The existence of at least two very different types of complexes was also reported by other authors [35].

### 3.2. Dst-3 induced conformational changes of calf thymus DNA

The  $\Delta y$  versus  $r$  curves of coil-like (*h*) and more rod-like (*l*) calf thymus DNA molecules reflect the relative changes of persistence length and contour length,  $\Delta a/a^0$  and  $\Delta L/L^0$ , in a different manner [14,18,23,36]. The change of both parameters was evaluated by means of eqs. (2a,b) as a function of  $r$  (fig. 2).

In the range  $r < 0.08$  of very strong binding no significant change of DNA contour length could be observed ( $|\Delta L_{1Dst}| < 0.03$  nm). On the other hand, after an initial increase at  $r < r_0 \approx 0.015$ , the persistence length drops in a manner which is, according to fig. B-1d, typical of a local-bending mechanism. (A Dst-induced  $\Delta L/L^0$  rise of about 11%, as found by measuring electric dichroism at 0.0025 M Na<sup>+</sup> [20], would implicate a  $\Delta y$  contribution of about 0.25 for the DNA

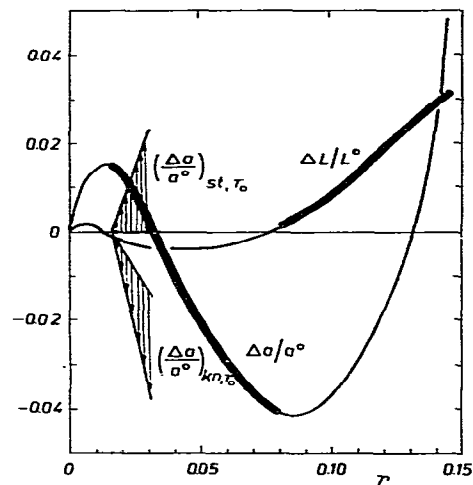


Fig. 2. Relative changes of DNA persistence length and contour length,  $\Delta a/a^0$  and  $\Delta L/L^0$ , as a function of  $r$ , evaluated from the two  $\Delta y(r)$  curves of fig. 1 by means of eqs. (2a, b). According to the criteria of appendix B and fig. B-1d, the descending part of the  $\Delta a/a^0$  versus  $r$  curve up to  $r \approx 0.08$  has to be correlated with a bending process. The slope of the local-bending increment,  $[d(\Delta a/a^0)_{kn}/dr]_{r_0}$  at  $r_0 = r$  (hatched interval) follows, according to eq. (B-1), from the slope of the experimental curve,  $[d(\Delta a/a^0)_{exp}/dr]_{r_0}$  and plausible limiting assumptions for the slope of the positive stiffening increment,  $[d(\Delta a/a^0)_{st}/dr]_{r_0}$  (hatched interval; estimated in analogy to DNA-netropsin interaction [14]); cf. text and table 1.

sample *l*, compared to the experimental value of 0.01 at 0.2 M Na<sup>+</sup> (fig. 1). It can be supposed that the very strong increase of contour length found experimentally for native DNA at low ionic strength [20a] contributes to the high Dst-induced elongation effects observed at 0.0025 M Na<sup>+</sup> by means of electric dichroism.)

The interaction mode at  $r > 0.08$  is characterized by (i) a considerable lower binding strength (section 3.1), (ii) a significant increase of DNA contour length, and (iii) a concomitant high increase of  $\Delta a/a^0$  to be explained by a strong DNA stiffening. For further interpretation see sections 3.7 and 3.8.

### 3.3. Dst-3 interaction with DNA of different base composition

In a previous paper [19] we published  $\Delta y$  versus  $r_t$  curves for almost coil-like DNA molecules with 69, 58, and 28 mole % (A+T), also measured at 0.2 M Na<sup>+</sup>.

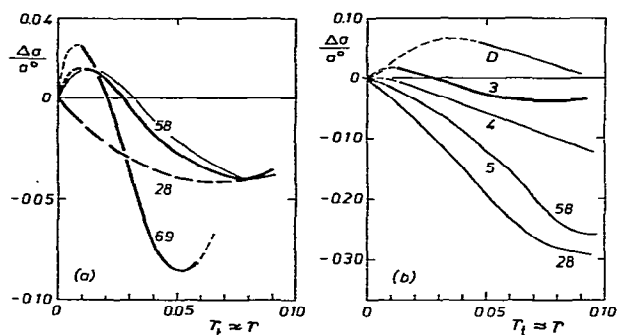


Fig. 3. (a) Relative changes of DNA persistence length as a function of  $r$  for Dst-3 interaction with coil-like DNA molecules of different (marked) A+T content and (b) for the distamycin derivatives Dst-D, Dst-3, Dst-4, Dst-5 with calf thymus DNA (58 mole % A+T) and for Dst-5 with DNA of 28% (A+T). For the evaluation of  $\Delta a/a^0$  from eq. (2c) see the text. (Thin line in (a):  $\Delta a/a^0$  versus  $r$  dependence from fig. 2.)

The results of the present paper and of appendices A and B permit a quantitative analysis. In analogy to the Dst-3 interaction with calf thymus DNA we are able to assume, for the range  $r < 0.05 \dots 0.08$ , a very strong ligand binding and a negligible change of contour length. Consequently, we can estimate the change of persistence length by means of eq. (2c) with the  $K_a$  values of table 1. The results are plotted in fig. 3a. The typical local-bending behaviour of  $\Delta a/a^0$  as explained in fig. B-1 is found for *Str. chrysomallus* DNA with 28% A+T. For the more (A+T) rich DNA species this  $\Delta a/a^0$  drop follows at  $r \gtrsim r_0$  after a small range of dominating stiffening (details in sections 3.5 and 3.6).

### 3.4. DNA interaction with Dst derivatives of different chain length

For Dst ligands with higher number of methylpyrrole rings the drop of DNA viscosity was shown to increase too [19]. With the same evident assumptions made in the preceding paragraph we get the  $\Delta a/a^0$  versus  $r$  curves depicted in fig. 3b for Dst derivatives with three, four and five rings and for a 3-ring Dst without the terminal C=O group (Dst-D). The character of the curves is again typical for ligand-induced local bending at not too low  $r$  values. With increasing ligand length the  $\Delta a/a^0$  versus  $r$  curves correspond to those expected for greater bending angles  $\gamma$  (fig. B-1d).

Table 1

Bending angles ( $\gamma$ )<sub>0</sub> and differences  $\Delta\lambda$  in the length of the complementary binding patterns of ligand and DNA ("mismatch") for the DNA-distamycin systems discussed. Other quantities derived and required are also listed (cf. text and footnote)

Ligand	DNA	[A+T] mol %	$\frac{M}{10^6}$	$K_a$	$100r_0$	$\left[\frac{d}{dr}(\Delta a/a^0)_{\text{exp}}\right]_{r_0}$	$\left[\frac{d}{dr}(\Delta a/a^0)_{\text{st}}\right]_{r_0}$	$\left[\frac{d}{dr}(\Delta a/a^0)_{\text{km}}\right]_{r_0}$	$\gamma_0/\text{degr}$	$\frac{\Delta\lambda/\text{nm}}{n}$	$\frac{\Delta\lambda/\text{nm}}{n+1}$	$\frac{\Delta\lambda/\text{nm}}{n+2}$
Dst-3	calf thym.	58	12.5	1.19 <sub>5</sub>	1.5	-(0.9...1.2)	+1.3...0	-(2.5...0.9)	6.3 ± 1.6	0.13 ± 0.03	0.04 <sub>3</sub>	0.03 <sub>2</sub> (0.02 <sub>5</sub> )
Dst-3	<i>Str. chrys.</i>	28	20	1.25	0.0	-1.3	1.0...0	-(2.3...1.3)	6.6 ± 0.9	0.13 ± 0.02	0.04 <sub>4</sub>	0.03 <sub>3</sub> (0.02 <sub>6</sub> )
	<i>Cl. perfr.</i>	69	7	1.13	1.1	-(1.9...2.6)	2.0...0	-(4.6...1.9)	8.8 ± 2.0	0.18 ± 0.04 (0.05 <sub>5</sub> )	0.04 <sub>4</sub>	0.03 <sub>3</sub>
Dst-4	calf thym.	58	20	1.25	1.0	-1.5	2.0...0	-(3.5...1.5)	7.5 ± 1.4	0.15 ± 0.03	0.04 <sub>0</sub>	0.03 <sub>0</sub> (0.02 <sub>4</sub> )
Dst-5	calf thym.	58	20	1.25	0.3	-2.3	2.5...0	-(4.8...2.3)	9.2 ± 1.6	0.18 ± 0.03	0.04 <sub>1</sub>	0.03 <sub>1</sub> (0.02 <sub>5</sub> )
	<i>Str. chrys.</i>	28	20	1.25	0.0	-3.4	2.0...0	-(5.4...3.4)	9.5 ± 2.0	0.20 ± 0.04	0.04 <sub>5</sub>	0.03 <sub>4</sub> (0.02 <sub>7</sub> )
Dst-D	calf thym.	58	18	1.24	4.3	-1.2	1.0...0	-(2.2...1.2)	6.4 ± 1.0	0.13 ± 0.02	0.04 <sub>3</sub>	0.03 <sub>2</sub> (0.02 <sub>5</sub> )

\* A variation of  $a^0$  from 45 nm to 60 nm in the theoretical basis reduces the values of  $\gamma$  by approximately 15%; cf. the treatment of a related problem [14]. On the other hand, a positive deviation of  $\gamma_0$  from the listed data on account of an incorrectly estimated stiffening effect  $[d(\Delta a/a^0)/dr]_{r_0}$  seems to be more probable than a negative one. Hence, the influences of these two effects on  $\gamma$  should cancel each other partially.

### 3.5. Angles of local DNA bending

The drop of  $\Delta a/a^0$ , typical of a ligand induced DNA bending, was shown to begin at an  $r$  value  $r_0 > 0$  (figs. 2, 3). The theoretical background for a quantitative determination of the angle of local bending  $\gamma_{r_0}$  (at  $r = r_0 + 0$ ) from the  $\Delta a/a^0$  versus  $r$  dependence is given in appendix B (eqs. (B-1) and (B-4b)). The data required are listed in table 1 for all the systems treated in sections 3.3 and 3.4. What we want to know is the initial slope of the "local-bending function"  $(\Delta a/a^0)_{kn}$  versus  $r$  at  $r_0 \leftarrow r$ . According to eq. (B-1) (also applicable to the derivative) it has to be estimated from the experimentally derived value  $[d(\Delta a/a^0)_{exp}/dr]$  after subtraction of the stiffening increment  $[d(\Delta a/a^0)_{st}/dr]$ . Estimated intervals for the two quantities are listed in table 1 for the different Dst-DNA systems. The intervals proposed for the stiffening increment were derived from the quantitative experience with related DNA netropsin systems [14]. The breadth of the resulting relative interval for  $\gamma_{r_0}$  (table 1) is comparatively small owing to the square-root character of eq. (B-4b). Analogous to DNA-netropsin interaction a base-sequence dependence of the Dst interaction has to be expected. It should implicate a non-constancy of  $\gamma$  with increasing  $r$  (cf. appendix B).

### 3.6. Model of DNA bending

Distamycin, like netropsin, associates specifically to DNA by hydrogen bonds. The amide groups of the oligopeptide as donors interact with the C(2)=O group of thymine or with N(3) of adenine [13,37–39]. This would only be possible without helix deformation if the lengths of the two binding patterns coincide. For netropsin interaction with very (A+T) rich DNA sequences the differences in the distances between the complementary groups of netropsin and of DNA implicate a local increase of DNA contour length [14,18]. This case is obviously not realized in DNA-Dst-3 complexes at 0.2 M Na<sup>+</sup> (cf. also [19]). A conceivable alternative would be the fixation of local helix curvature since the acceptor groups of DNA are arranged in a finite distance from the helix axis. Due to the statistical structural fluctuations the local helix curvature accepts comparatively high values and the mutual distances between the DNA-own acceptor groups concomitantly change. This may be a situation suitable for an

in-register binding of a ligand equipped with a pattern of hydrogen donors of different distances. The hydrogen bonds of the DNA-Dst complex are formed step by step [39a]. From model considerations [40] and unpublished investigations it has to be concluded that the Dst-own binding pattern is the longer one.

A scheme given in figs. 4a, b demonstrates the most fundamental features of this model. In oversimplification of the problem the backbones of the two components are drawn parallel. A "mismatch"  $\Delta\lambda$  is defined by fig. 4a. It is to represent the maximum difference between the effective lengths of donor and acceptor patterns. (For both we draw equal distances between all their links to simplify matters.) In this case the equation which relates  $\Delta\lambda$  with the distance between the ligand backbone and the polymer axis,  $\Delta R$ , and the bending angle  $\gamma$  is very easily derived to  $\gamma = \Delta\lambda/\Delta R$ .

For the more realistic case of a short linear ligand associated parallel to one DNA strand we have to consider the pitch angle  $\beta$  (fig. 4c). In the limits of our elementary model only the  $\Delta\lambda$  component parallel to the helix axis is effective in bending the polymer. Consequently,  $\gamma = \Delta\lambda \sin \beta / \Delta R$  or

$$\Delta\lambda = \Delta R \gamma / \sin \beta. \quad (4)$$

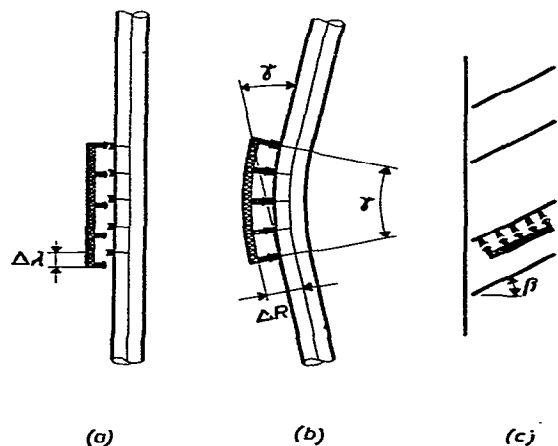


Fig. 4. (a, b) Rough schematic model for local polymer-bending by in-register formation of (hydrogen) bonds to a ligand hypothetically aligned parallel to the polymer axis with a distance  $\Delta R$  between their backbones (cf. text). (c) For the realistic case of short linear ligands bound in the small DNA groove parallel to one DNA strand the existence of a pitch angle  $\beta < \pi/2$  modifies the geometric relations (cf. text and eq. (4)).

With  $\beta \approx 35^\circ$  and  $\Delta R \approx 0.65$  nm we get the mismatch values  $\Delta\lambda$  as listed in table 1.

What we are interested in is the mismatch per base pair,  $\Delta\lambda_{bp}$ . If  $n$  is the number of methylpyrrole rings per Dst molecule (cf. fig. 1) the maximum number of potential hydrogen bonds to adjacent DNA monomer units is  $(n+2)$ . Resulting from DNA base sequence usually not all limiting possibilities are expected to be realized. Therefore, table 1 contains the data for  $\Delta\lambda/(n+2)$ ,  $\Delta\lambda/(n+1)$  and  $\Delta\lambda/n$ . One of these values should represent  $\Delta\lambda_{bp}$ . Respective data are in surprisingly good accord for all systems considered, with the only exception of the values for the DNA species of the highest (A+T) content. This system obviously and reasonably forms one more hydrogen bond at  $r \approx r_0$ . This consistency of the values supports the essential features of the model applied. The mismatch per base pair,  $\Delta\lambda_{bp}$ , amounts to  $(0.032 \pm 0.008)$  nm or, perhaps,  $(0.043 \pm 0.01)$  nm, and the corresponding bending angle per base pair,  $\gamma_{bp}$ , results in  $(1.6 \pm 0.4)^\circ$  or  $(2.1 \pm 0.5)^\circ$ .

### 3.7. Two lines of Dst-3, bound side by side in the small groove

At  $r > 0.08$  binding of the non-intercalating ligand Dst-3 induces an increase of DNA contour length, after fig. 2 and eq. (3) of about  $\Delta L_{1D\&3} = 0.08$  nm. This result is in qualitative accord with the rather small helix unwinding to be derived, in *this*  $r$ -range, from sedimentation experiments on superhelical DNA [34,41]. In view of the following arguments both effects can be understood by a model of side-by-side binding of Dst-3 inside the narrow groove and parallel to both DNA strands.

Experimental [42] and theoretical [43] investigations on DNA secondary structure have generally shown that increase of DNA contour length and broadening of the small groove are coupled processes. An association of linear Dst molecules in a second line should cause, for stereochemical reasons, a broadening of the narrow groove. This effect, consequently, is expected to be accompanied by an increase of DNA contour length, as experimentally observed. For the other DNA-Dst systems treated in this paper, the potential validity of the two-lines model is supported by similarities in the viscosity behaviour of DNA at high  $r$  values [19]. Zimmer and Luck [44] proposed this

binding type in interpreting CD measurements upon Dst-5 interaction with poly [dA-io<sup>5</sup>dU] · poly [dA-io<sup>5</sup>dU], a polynucleotide with bulky substituents in the large groove. Since Dst binding in the deep groove must be excluded from stereochemical reasons, the existence of a rather strong Dst association at high  $r$  values is understandable if we accept the model presented.

### 3.8. DNA stiffening

The  $\Delta a/a^0$  increase of DNA, observed on Dst-3 interaction at  $r < r_0 = 0.015$  and  $r > 0.1$ , indicates the prevailing of a stiffening effect. Dst-DNA complexes locally form "triple helices" like netropsin-DNA systems [14,18] or even "quadruple helices" (section 3.7). Of course, the constraints between ligand and polymer partially freeze helix-internal degrees of freedom resulting in a stiffening increment of  $\Delta a/a^0$ .

To study details of the interaction mechanism at  $r < r_0$  preliminary measurements were performed at different temperatures and with  $\text{NH}_4^+\text{DNA}^-$ . The results can scarcely be understood without assuming in (A · T) clusters *small* local deviations from the average DNA B-conformation (cf. also [14,44a]). Titration viscometric investigations on DNA interactions with oligopeptide antibiotics provide a sensitive difference method to study local changes of DNA secondary structure. Further investigations are in progress.

## 4. Biological implications

The Dst-induced local-bending angle per DNA base pair,  $\gamma_{bp}$ , implicates a radius of local helix curvature near 10 nm, independent of the DNA and Dst species. This effect is the result of a small distinct difference in the length patterns of the complementary components. The radius approaches that in nucleosomes with-in a factor of approximately two [45]. This example demonstrates the general ability of peptide compounds to generate a helix curvature, and it cannot be excluded that related mechanisms of histone interaction are involved in nucleosome formation. Also the viscosity response of DNA on interaction with both L-lysyl-L-phenyl-alaninamide and L-lysyl-D-phenyl-alaninamide [46] has to be considered characteristic of a dominating ligand induced local bending or kinking ef-

fect. This aspect again illuminates a potential role of aromatic amino acids in specific DNA-protein interaction. Another example exhibits the DNA-actinomycin system treated in appendix C.

Recently, Hogan et al. [20] reported on "transmission of allosteric effects in DNA" as a consequence of Dst binding. This ligand binds co-operatively at very low  $r$  values under low and high salt concentrations. The very large elongation effect observed at 0.0025 M  $\text{Na}^+$  was not found at 0.2 M  $\text{Na}^+$  (cf. section 3.2). Nevertheless, a mechanism of in-register association due to constraints between the components may be [20a] in line with the essential features of those results.

Binding of the peptide antibiotics Dst and netropsin is (A · T) cluster specific [14]. On the other hand DNA binding sites for regulatory proteins usually are characterized by a higher than average (A+T) content [47]. Hence, studies about interaction of Dst and netropsin with DNA enable us to learn some details about elementary steps of specific interaction which may be of interest in understanding protein-DNA recognition. Evidence for two-line binding of Dst along the narrow groove, e.g., is of interest [48] in context with some current models of protein-DNA recognition, which suggest the binding of  $\beta$ -ribbons in the small groove [49,2,3].

## Acknowledgement

The author is indebted to Drs. F. Arcamone and Ch. Zimmer and to Dipl. Chem. Eva Sarfert for the gifts of distamycin and DNA, respectively, and to Mrs. Dörthe Geller for technical assistance. Thanks for computer programming and calculations are due to Dipl. Math. D. Hellmich (Berlin-Buch), Dr. Eberhard Stutter, the computer group of this institute and Chem. Ing. H. Bär. For fruitful discussions, encouragements and critical reading of parts of the manuscript I thank Prof. H. Berg, Drs. Ch. Zimmer, K. Geller, H. Triebel, G. Luck, E. Stutter and W. Förster. The author is indebted also to a referee. The reply to his questions required the addition of appendix C. The main part of the paper was presented at the XIIth FEBS Meeting in Dresden, 1978.

## Appendix A

### *The persistence length of worm-like chain molecules with locally enhanced flexibility*

Characteristic quantities describing the effective flexibility of worm-like chain polymers are the Kuhn statistical segment length or the persistence length  $a$ . Local increase of flexibility and local bending reduce the size of the molecules. A theoretical description of this phenomenon should consider the deviation of the chain dimensions from those of the undisturbed molecule. An approximation was given by Gray and Hearst [50] with the concept of a worm-like chain with universal joints. To describe the influence on chain flexibility of both rotational isomerism and torsional oscillations within each isomer Birshtein found the equation [51,52]

$$1/a = 1/a_{\text{ri}} + 1/a_{\text{to}} \quad (\text{A-1})$$

The two (reciprocal) persistence lengths of its right-hand side describe the case that rotational isomerism or torsional oscillations, respectively, are the only mechanisms responsible for chain flexibility.

Here we intend to demonstrate, in a general manner, that an equation of this type describes the influence of any two contributions to polymer flexibility. Let us, therefore, consider three model chains of equal length and different gross flexibility, similar to that treated by Kratky and Porod [53] as a prestage to the worm-like chain. The length of their discrete links differ in a suitable manner as described below and the mean angles  $(\alpha^2)^{1/2}$  between adjacent elements are supposed to be (i) small  $((\alpha^2)^{1/2} \ll 1)$  and (ii) the same between all the links for the three chains. Chain C (fig. A-1) represents a polymer model with stiff elements of equal length  $\lambda$ . Chains A and B are constructed in such a way that chain C contains the flexible joints of chain A and chain B. For chain B, therefore, always  $p$  of any  $q$  joints of chain C are fixed to form longer co-linear model links. For chain A the complementary  $(q-p)$  of  $q$  joints are to be immobilized. In fig. A-1,  $q = 3$  and  $p = 1$ . The properties of these three polymer models, in particular after reaching the limit ( $\lambda \rightarrow 0$ ) of a worm-like chain, can be correlated by the well-known relation [53]

$$\overline{\cos \psi} = \exp(-L/a) \quad (\text{A-2})$$



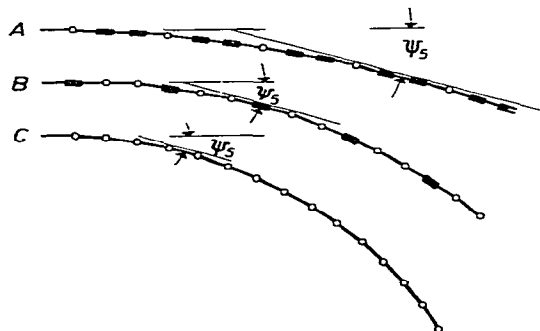


Fig. A-1. Schematic representation of eq. (A-2), in particular of its prestage before passing to the worm-like-chain limit of vanishing element length [53], for two model chains (A,B) with differing number of flexible joints and one chain (C) involving the joints of both chain A and chain B (cf. text).  $\psi_5$  is the mean direction of the fifth chain elements relative to that of the respective first ones.

used also as a definition of persistence length  $a$  [54]. In this equation  $L$  may be considered as a curvi-linear coordinate, and  $\psi$  is the angle between the tangents to the molecule axis at  $L$  and at  $L = 0$ .  $\overline{\cos \psi}$  is the average of  $\cos \psi$  over all possible configurations.

For our considerations it is important that, according to the supposition of equal  $\overline{\alpha^2}$ , the same value of  $\overline{\cos \psi}$  will be realized by chain segments having the same number  $\mu$  of links (in fig. A-1,  $\mu = 5$ ). On the other hand, eq. (A-2) (or the corresponding relation for chains with links of discrete length [53]) demands equal values of  $L/a$  for segments with equal number of linear elements. This means that for the three chains considered  $a$  is proportional to the mean element length. With  $a_C$ ,  $a_B$ , and  $a_A$  being the effective persistence lengths of the three chains, therefore, we get

$$a_A = (q/p) a_C, \quad a_B = [q/(q-p)] a_C. \quad (\text{A-3a, b})$$

These two equations, valid for sufficient long chains, evidently fulfil the relation

$$1/a_C = 1/a_A + 1/a_B. \quad (\text{A-4a})$$

This is the result we were looking for. According to the general form of the model used eq. (A-4a) describes the additivity of any different contributions to polymer flexibility.

For application of eq. (A-4a) to DNA with a *locally*

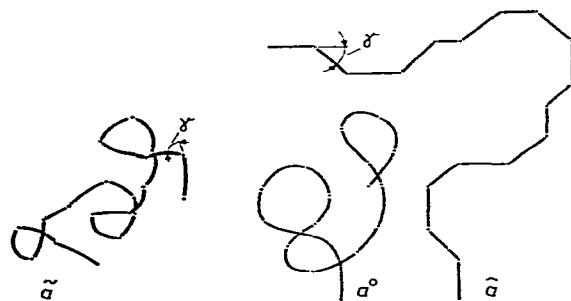


Fig. A-2. The persistence length  $a^0$  of a worm-like chain molecule may be reduced to  $a$ , e.g. by setting of (ligand induced) kinks (or by local increase of flexibility). In this case  $\tilde{a}$  and  $a^0$  are related by eq. (A-4b).  $\tilde{a}$  is the apparent persistence length of a rigid-polymer model of the same length like the original molecule. This model, however, exhibits the structure *modification pattern* transforming  $a^0$  to  $\tilde{a}$ .

*enhanced effective flexibility* it is appropriate to correlate  $a_C$ ,  $a_A$ , and  $a_B$  with the persistence lengths of this “modified” DNA molecule,  $\tilde{a}$ , of the undisturbed polymer,  $a^0$ , and of a rigid molecule model of equal length provided with the same structural “modification” pattern,  $\tilde{a}$ , respectively:

$$1/\tilde{a} = 1/a^0 + 1/\tilde{a}. \quad (\text{A-4b})$$

For locally bent or kinked DNA these three chains are represented in fig. A-2. Before any alteration of the geometrical properties of the “native” DNA molecule  $\tilde{a} = \infty$ . (Further mechanisms causing an additional decrease of persistence length require, in eq. (A-4b), the addition of respective terms  $1/\tilde{a}_i$ .)

An experimentally observed relative decrease of persistence length  $(\Delta a/a^0)_d = (\tilde{a} - a^0)/a^0$ , stemming from an effective increase of flexibility by action of one process only, depends on  $\tilde{a}$  in a very simple manner. With eq. (A-4b) it follows very easily

$$(\Delta a/a^0)_d = -a^0/(\tilde{a} + a^0). \quad (\text{A-5a})$$

For small structural changes ( $a^0 \ll \tilde{a}$ ) we can write

$$(\Delta a/a^0)_d = -a^0/\tilde{a}. \quad (\text{A-5b})$$

(The effect of two the persistence length reducing processes is described analogously by  $(\Delta a/a^0)_d = -a^0/\tilde{a}_1 - a^0/\tilde{a}_2$ .) A theoretical expression for  $\tilde{a}$  in terms of the

angle  $\gamma$  of ligand induced kinking or local bending and the (low) degree of ligand binding,  $r$ , is given in eq. (B-3b).

The quantitative interpretation of local-stiffening effects is described elsewhere [14,18,36] and considered in appendix B.

## Appendix B

### Change of apparent DNA persistence length by discrete local bends or kinks

Complex formation of DNA molecules with low molecular weight ligands may be accompanied by the formation of local helix bends. The determination of the bending angle  $\gamma$  is often of biological interest (cf. also [55–57]). A quantitative investigation of the kinking angle, i.e. of local bending occurring only between two base pairs, has been performed by X-ray analysis of complexes between self-complementary dinucleotide mini-helices and drugs [58–60]. Related estimates have been published for irhediamine complexes with rod-like DNA helices at very low ionic strength. The authors measured an increase of base tilting by means of transient electric dichroism [57].

Here we deal with the (measurable) change of DNA persistence length by ligand induced local bending. As to be shown, its relative change  $\Delta a/a^0$  varies with the degree of binding  $r$  (= concentration ratio of bound ligand and DNA phosphate) in a very characteristic manner. This typical behaviour enables us to calculate the angle of local bending,  $\gamma$ .

#### B.1. Characteristic changes of DNA persistence length by local bends

By means of eqs. (A-4b, A-5b) the conformational statistical considerations for DNA with enhanced effective flexibility can be simplified considerably. For DNA molecules with local bends solely a rigid and originally straight model helix of the same contour length and supplied with the same kinking pattern has to be treated. Local bending of duplex DNA reduces its end-to-end distance (fig. B-1a) and, consequently, its effective persistence length. Generally, its ligand-induced relative change,  $\Delta a/a^0$ , can be caused by two increments of different origin. These are (i) a contri-

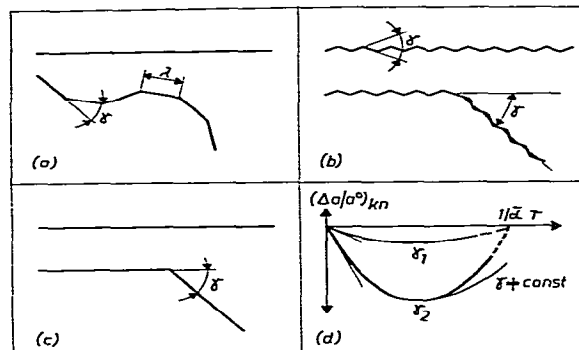


Fig. B-1. Illustration of the relative change of DNA persistence length by regular, ligand-induced distinct local bends. Due to eqs. (A-5a, b), only the behaviour of equivalent rigid linear polymer models with identical local-bending patterns needs to be considered (cf. fig. A-2). (a) Local-bending reduces the end-to-end distance of the polymer and, consequently, the effective persistence length;  $\gamma$  is the bending angle,  $\lambda$  is the distance between two bound DNA-bending ligands. (b, c) For DNA molecules, saturated by a hypothetical maximum number  $m_{\max}$  of bound and local-bends (kinks) inducing ligands, and for "naked" DNA molecules both the external shape and the hydrodynamic behaviour should be almost equivalent. The same should hold true, on average, for corresponding molecules with  $(m_{\max} - \nu)$  and  $\nu$  kinks ( $\nu = 1, 2, 3, \dots$ ). This symmetry property is a consequence of the correlation between the distance  $\lambda$  of adjacent bending ligands and the spatial bending direction  $\Theta$ . It results in "local-bending functions"  $(\Delta a/a^0)_{kn}$  versus  $r$  similar to those represented in (d) for different local-bending angles,  $\gamma_1$  and  $\gamma_2$ .  $\bar{\alpha}$  is the number of nucleotides per binding site. For details and limitations see the text.

bution of local stiffening,  $(\Delta a/a^0)_{st}$ , and (ii) a negative increment of distinct local bending,  $(\Delta a/a^0)_{kn}$

$$\Delta a/a^0 = (\Delta a/a^0)_{st} + (\Delta a/a^0)_{kn}. \quad (B-1)$$

The discrimination between both contributions requires additional criteria. For a schematic illustration by means of two-dimensional graphs (fig. B-1) we consider regular  $\epsilon$ -bends in the nomenclature of Sobel et al. [56]. (This means that the simplified model regards binding of DNA-bending ligands in a mutual distance of half a pitch.)

Now, let us compare an uncomplexed DNA molecule (fig. B-1c), above) with a second one the binding sites of which are covered by a stereochemically maximum number  $m_{\max}$  of helix-bending ligands (fig. B-1b). For small bending angles  $\gamma$  the radius of gyra-

tion and the hydrodynamic behaviour of both models should roughly be equivalent. The same should be valid for  $(m_{\max} - \nu)$  and  $\nu$  bound bending ligand molecules, respectively ( $\nu = 1, 2, \dots$ ; see, for  $\nu = 1$ , figs. B-1b,c). Consequently, for our idealized model the dependence of  $(\Delta a/a^0)_{kn}$  on  $r$ , here called local-bending function, should be symmetrical and nearly of the type presented in fig. B-1d for two different bending angles  $\gamma_1$  and  $\gamma_2 > \gamma_1$ .

Local-bending functions of real systems should differ from the ideal one by a loss of symmetry. This tendency is caused by the rules of statistical ligand binding [61,62] and, for ligands of the distamycin type, also by the DNA base sequence and a concomitant possible inconstancy of  $\gamma$ . *Characteristic* features of a local-bending function  $(\Delta a/a^0)_{kn}$  versus  $r$  are the drop at low  $r$  values and the following *continuous diminution of the negative slope*. This should be valid also for non- $\epsilon$  bends.

### B.2. Change of persistence length and angle of local bending, $\gamma$

The criteria discussed in section B.1 enable us to decide whether or not a local bending effect exists. As long as experimental methods do not permit an exact discrimination between the two increments  $(\Delta a/a^0)_{kn}$  and  $(\Delta a/a^0)_{st}$  of eq. (B-1), limiting assumptions about the latter quantity have to be made to get a reasonable interval for  $(\Delta a/a^0)_{kn}$ . (The error of  $\gamma$  resulting from this procedure is comparatively low owing to the square-root character of the decisive eq. (B-4b) below.)

Due to eq. (A-5b) and fig. A-2 now we only have to derive an expression which relates the effective *persistence length  $\bar{a}$  of a rigid but bent helix* to the bending angle  $\gamma$ . This shall be done in three steps.

(i) The mean value  $\bar{\lambda}$  of the length  $\lambda$  (fig. B-1a) between two bends is the average of the distance between two bound ligand molecules.

$$\bar{\lambda} = h/2r \quad (\text{B-2})$$

( $h$  is the translation per base pair, 0.34 nm for B-DNA).

(ii) The angle of the spatial bending direction  $\Theta$  is governed by the DNA helix geometry and the distance of adjacent bound ligands. (Both planes, defined by the linear segments which generate two adjacent helix bends ( $j, k$ ), form an azimuthal angle  $\Theta = 2\pi\lambda_{jk}/p$ ;  $\lambda_{jk}$  is the distance between these bends; cf. fig. B-1d, [30].)

For sufficiently high  $\lambda_{jk}$  (low  $r$ ) values the correlation between  $\Theta$  and  $\lambda$  can be neglected.

(iii) Let us consider a Kratky and Porod chain [53] with rigid linear elements of the length  $\bar{\lambda}$ . These elements may be linked in such a manner that *all* directions between adjacent elements, forming the same *small* angle  $\bar{\gamma}$ , are realized with the same probability. The persistence length  $\bar{a}$  of this chain is given [53] by the equation

$$\bar{a} = 2\bar{\lambda}/\bar{\gamma}^2. \quad (\text{B-3a})$$

Ligand induced local bends, however, can only be realized into *one* azimuthal direction  $\Theta$ . If  $\sin^2\gamma \ll \cos^2\gamma \approx 1$  it can be shown by matrix methods [63,64] that eq. (B-3a) is a good approximation for locally bent DNA, too. (Note, that at present the accuracy in the separation of both  $\Delta a/a^0$  increments of eq. (B-1) is limited.) Therefore, we can write  $\bar{a} = 2\bar{\lambda}/\gamma^2$  and together with eq. (B-2),

$$\bar{a} = h/(r\gamma^2) \quad (\text{B-3b})$$

With eq. (A-5b), applied to the local-bending increment of the relative change of persistence length,  $(\Delta a/a^0)_{kn}$ , we get for very small  $r$  values

$$\gamma^2 = - \frac{(\Delta a/a^0)_{kn}/r}{a^0/h}. \quad (\text{B-4a})$$

$(\Delta a/a^0)_{kn}/r$  is to be understood as the slope  $d(\Delta a/a^0)_{kn}/dr$  of the  $(\Delta a/a^0)_{kn}$  versus  $r$  dependence for very small  $r$  values ( $0 \leftarrow r$ ). Generally, for the beginning of the bending process at  $r_0$  we have to write

$$\gamma = \left\{ - \left[ \frac{d(\Delta a/a^0)_{kn}/dr}{a^0/h} \right]_{r_0 \leftarrow r} \right\}^{1/2}. \quad (\text{B-4b})$$

## Appendix C

### DNA-actinomycin interaction

Sobell et al. assume a local bending of DNA due to actinomycin (Acm) binding [56]. This result can also be derived from hydrodynamic data. In a pioneer work by Müller and Crothers, a viscometric investigation of DNA-Acm interaction was carried out at physiological salt concentrations on several DNA samples of different molecular weight between  $M = 10^5$  and  $10^8$  [65].  $[\eta]$  rises for very short and decreases for

larger molecules. In a first interpretation the occurrence of a DNA elongation (intercalation) and intramolecular chain-chain interactions was proposed. (To explain the drop of viscosity observed upon DNA-Dst complex formation, chain-chain interaction had also been assumed years ago by this author [66].)

In the light of later experience, three independent arguments in favour of a mechanism different from chain-chain interaction have to be considered. (i) Viscosity experiments with coil-like DNA molecules at very low ionic strength (0.005 M Na<sup>+</sup>) exhibit a similar viscosity drop upon Dst or Acm interaction [67]. At this salt concentration close chain-chain contacts are improbable. (ii) In 0.2 M Na<sup>+</sup> a diminished viscosity rise exists already at very short molecules ( $M = 0.23 \times 10^6$ ) [65], for which intramolecular chain-chain interactions cannot be expected. (iii) If thermodynamic conditions permit chain-chain associations of different polymer segments, association between different molecules is possible, too. Such an effect would enhance the concentration dependence of viscosity considerably. No influence has been observed, however, for the high molecular weight DNA sample of the systems DNA-Dst (fig. 1) and DNA-Acm [67].

Another explanation for the hydrodynamic behaviour of the DNA-Acm system would be the assumption of a ligand induced rise of DNA contour length coupled with a drop of persistence length (see fig. 1 in [14]). This was mentioned already in [65]. In order to check this hypothesis the interpolated experimental  $\Delta\gamma = \Delta[\eta]/[\eta]^0$  versus  $r$  data [65] were tentatively analysed in terms of  $\Delta L/L^0$  and  $\Delta a/a^0$ . Four different couples of high and low molecular weight calf thymus DNA samples were combined, and the second order approach was applied analogously to eqs. (2a,b) with adapted parameters [23]. A rise of the effective DNA helix diameter by ligand association was also considered. (To prevent systematic errors, caused by the excluded volume effect and by differences in DNA base composition, the T2 phage DNA data were not taken into consideration.) Fig. C-1 shows the relative change of DNA contour length and of DNA persistence length calculated in dependence on  $r \equiv r_p$  (or  $r_{bp} = 2r_p$ , the abscissa used in [65]). The vertical dimensions of the  $\Delta L/L^0$  symbols approximately correspond to the interval resulting from estimation or neglect of helix diameter changes. For  $\Delta a/a^0$  this influence is negligible.

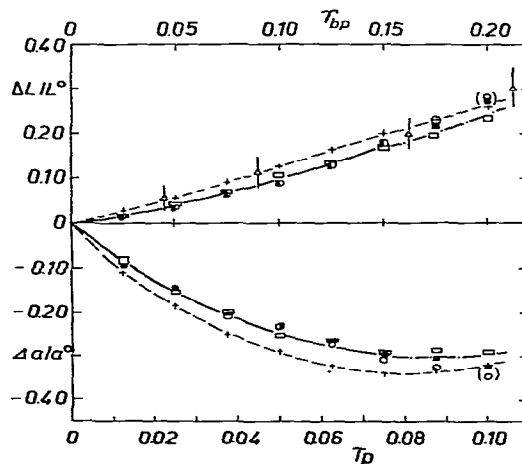


Fig. C-1. Relative change of DNA persistence length and contour length,  $\Delta L/L^0$  and  $\Delta a/a^0$ , as a function of  $r$  ( $\equiv r_p = 2r_{bp}$ , moles Acm bound per mole DNA Phosphate or base pair, respectively). Calculations were performed as described in the text using experimental data from literature ([65]; combinations of different DNA samples:  $\square M/10^6: 0.52/26$ ;  $\blacksquare 0.23/26$ ;  $\circ 0.23/1.3$ ;  $+$   $0.1/1.3$ ;  $\triangle$  values derived from the  $M = 0.1 \times 10^6$  data [65]).

The  $\Delta L/L^0$  and  $\Delta a/a^0$  values, derived from different DNA sample combinations with molecular weights between  $0.23 \times 10^6$  and  $24 \times 10^6$ , are in best mutual accord. If the DNA sample  $M = 0.1 \times 10^6$  is considered the  $\Delta L/L^0$  values calculated are different from those obtained from other  $M$  combinations. Those  $\Delta L/L^0$  values, however, agree with the data calculated only from the viscosities of the  $M = 0.1 \times 10^6$  DNA sample by means of a rigid particle model [65] (fig. C-1). Due to the agreement of the data for three  $M$  combinations and the particular character of the deviations for the fourth, we believe the full lines in fig. C-1 to describe the Acm induced DNA conformational changes in a comparatively correct manner. The coincidence of the data, obtained for different independent calculations, also suggests the adequacy of the underlying theoretical background.

The shape of the  $\Delta a/a^0$  versus  $r$  curve in fig. C-1 is typical for a ligand induced local DNA bending or kinking (fig. B-1 d). Eqs. (B-4b) and (B-1) permit to calculate an apparent bending angle  $\gamma$ . The slope of the experimental  $\Delta a/a^0$  versus  $r$  curve at  $r \rightarrow 0$  is

$[d(\Delta a/a^0)_{\text{exp}}/dr]_{r \rightarrow 0} = -6.8$ . A reasonable limiting interval for the stiffening increment  $d(\Delta a/a^0)_{\text{st}}/dr_{r \rightarrow 0}$  is assumed to range from  $-2$  to  $+3$ . These values follow from a rough comparison of fig. C-1 with fig. B-1d on the one hand and the stiffening increments derived for netropsin-DNA interaction [14] on the other. With eq. (B-1) we obtain  $[d(\Delta a/a^0)_{\text{kn}}/dr]_{r \rightarrow 0} = -(4.8 \dots 9.8)$  and from eq. (B-4b)  $\gamma^2 = 0.036 \dots 0.074$ . Consequently, the Acm-induced apparent bending angle  $\gamma$  for calf thymus DNA lies between  $11^\circ$  and  $16^\circ$ . Owing to the magnitude of this interval the error resulting from the intrinsic assumption  $\gamma^2 \ll 1$  can be neglected. The  $\gamma$  value derived is smaller by a factor of about three to that reported for Acm-dinucleoside monophosphate interaction [56]. With regard to the constraints of adjacent nucleotides in the natural double helix and to the concept of telestability [68] the  $\gamma$  value derived seem to be a reasonable result.

## References

- [1] N.C. Seeman, J.M. Rosenberg and A. Rich, *Proc. Natl. Acad. Sci. USA* 73 (1976) 804.
- [2] G.V. Gursky, V.G. Tumanyan, A.S. Zasedatelev, A.L. Zhuse, S.L. Grokhovsky and B.P. Gottikh, *Molecular Biology Reports* 2 (1976) 413.
- [3] G.M. Church, I.L. Sussman and S.H. Kim, *Proc. Natl. Acad. Sci. USA* 74 (1977) 1458.
- [4] C. Héline, *FEBS-Letters* 74 (1977) 10.
- [5] P.H. von Hippel, in: *Biological regulation and development*, Vol. 1, ed. R.F. Goldberger (Plenum Publishing Corporation, 1979).
- [6] B. Puschendorf and H. Grunicke, *FEBS-Letters* 4 (1969) 355.
- [7] P. Chandra, Ch. Zimmer and H. Thrum, *FEBS-Letters* 7 (1970) 90.
- [8] U. Wähnert, Ch. Zimmer, G. Luck and Ch. Pitra, *Nucl. Acids. Res.* 2 (1975) 391.
- [9] Ch. Zimmer, in: *Progress in nucleic acids research and molecular biology*, Vol. XV, ed. W.E. Cohn (Academic Press, New York and London, 1975) p. 285.
- [10] R.M. Wartell, J.E. Larson and R.D. Wells, *J. Biol. Chem.* 249 (1974) 6719.
- [11] J.V. Smirnov and A.J. Poletaev, *Biofizika* 23 (1978) 384.
- [12] J.C. Martin, R.M. Wartell and D.C. O'shea, *Proc. Natl. Acad. Sci. USA* 75 (1978) 5483.
- [13] Ch. Zimmer, G. Luck, H. Lang and G. Burckhardt, *Proc. 12th FEBS-Meeting, Dresden 1978*, eds. S. Rosenthal et al., p. 83-94.
- [14] K.E. Reinert, E. Stutter and H. Schweiss, *Nucl. Acids Res.* 7 (1979) 1375.
- [15] G.V. Gursky, V.G. Tumanyan, A.S. Zasedatelev, A.L. Zhuse, S.L. Grokhovsky and B.P. Gottikh, in: *Nucleic acid protein recognition*, ed. H.I. Vogel (Academic Press, New York, 1977) p. 189.
- [16] H.M. Berman, S. Neidle, Ch. Zimmer and H. Thrum, *Biochim. Biophys. Acta* 561 (1979) 124.
- [17] Ch. Zimmer, K.E. Reinert, G. Luck, U. Wähnert, G. Löber and H. Thrum, *J. Mol. Biol.* 58 (1971) 329.
- [18] K.E. Reinert, *J. Mol. Biol.* 72 (1972) 593.
- [19] G. Luck, Ch. Zimmer, K.E. Reinert and F. Arcamone, *Nucl. Acids Res.* 4 (1977) 2655.
- [20] M. Hogan, N. Dattagupta and D.M. Crothers, *Nature* 278 (1979) 521.
- [20a] K. Geller and K.E. Reinert, *Nucl. Acids Res.* 8 (1980) 2807; K. Geller, thesis, University of Jena, 1978.
- [21] E. Sarfert and H. Venner, *Naturwiss.* 49 (1962) 423.
- [22] Ch. Tanford, *Physical chemistry of macromolecules* (J. Wiley, New York, 1961).
- [23] K.E. Reinert and K. Geller, *Studia Biophysica* 45 (1974) 1. (Reprints still available).
- [24] E.O. Kraemer, *Ind. Eng. Chem.* 30 (1938) 1200.
- [25] D.M. Crothers and B.H. Zimm, *J. Mol. Biol.* 12 (1965) 525.
- [25a] B.M.J. Revet, M. Schmir and J. Vinograd, *Nature New Biol.* 229 (1971) 10.
- [26] C.J. Halfman and T. Nishida, *Biochemistry* 11 (1972) 3493.
- [27] K.E. Reinert, *Biochem. Biophys. Acta* 319 (1973) 135.
- [28] C. Gatti, C. Houssier and E. Fredericq, *Biochim. Biophys. Acta* 407 (1975) 308.
- [29] C. Gatti, C. Houssier and E. Fredericq, *Biochim. Biophys. Acta* 476 (1977) 65.
- [30] J.A. Schellman, *Biopolymers* 13 (1974) 217.
- [31] H. Triebel, K.E. Reinert and J. Strassburger, *Biopolymers* 10 (1971) 2619.
- [32] J. Garcia de la Torre and A. Horta, *J. Phys. Chem.* 80 (1976) 2028.
- [33] G. Mazza, A. Gallizi, A. Minghetti and A. Siccardi, *Antimikrob. Ag. Chemother.* 3 (1973) 384.
- [34] G. Luck, H. Triebel, M. Waring and Ch. Zimmer, *Nucl. Acids Res.* 1 (1974) 503.
- [35] F. Zunino and A. DiMarco, *Biochem. Pharmacology* 21 (1972) 867.
- [36] K.E. Reinert, in: *Physico-chemical properties of nucleic acids*, Vol. 2, ed. J. Duchesne (Academic Press, London 1973) p. 319.
- [37] J.C. Martin, R.M. Wartell and D.C. O'shea, *Proc. Natl. Acad. Sci. USA* 75 (1978) 5483.
- [38] H.M. Berman, S. Neidle, Ch. Zimmer and H. Thrum, *Biochim. Biophys. Acta* 561 (1979) 124.
- [39] A.S. Krylow, S.L. Grokhovsky, A.S. Zasedatelev, A.L. Zhuse, G.V. Gursky and B.P. Gottikh, *Nucl. Acids Res.* 6 (1979) 289.
- [39a] J.V. Smirnov and A.J. Poletaev, *Biofizika* 23 (1978) 384.
- [40] G.V. Gursky, private communication.
- [41] M.J. Waring, in: *The molecular basis of antibiotic action* (Wiley, London, 1972) p. 173.

- [42] S. Arnott, R. Chandrasekaran and E. Selsing, in: *Structure and conformation of nucleic acids and protein-nucleic acid interaction*, eds. M. Sundaralingam and S.T. Rao (Baltimore, 1975).
- [43] V.B. Zhurkin, V.I. Lysov and V.I. Ivanov, *Biopolymers* 17 (1978) 377.
- [44] Ch. Zimmer and G. Luck, to be submitted.
- [44a] K.E. Reinert, E. Sarfert and H. Thrum, *Nucl. Acids. Res.*, in press.
- [45] G. Felsenfeld, *Nature* 271 (1978) 115.
- [46] E.J. Gabbay, P.D. Adawadkar and W.D. Wilson, *Biochemistry* 15 (1976) 146.
- [47] W. Gilbert, A. Maxam and A. Mirzabekov, in: *Control of ribosome synthesis*, eds. N.O. Kjeldgaard and O. Malvoe (Muksgaard, Copenhagen, 1976) p. 139.
- [48] M. Spencer, *Nature* 267 (1977) 579.
- [49] S.H. Kim, J.L. Sussman and G.M. Church, in: *Structure and conformation of nucleic acids and protein-nucleic acid interaction*, eds. M. Sundaralingam and S.T. Rao (Baltimore, 1975).
- [50] H.B. Gray Jr. and J.E. Hearst, *J. Mol. Biol.* 35 (1968) 111.
- [51] T.M. Birshtein, *Vysokomolek. Soedin.* 8 (1966) 168; 16A (1974) 54.
- [52] T.M. Birshtein and O.B. Ptitsyn, *J. Polym. Sci. C16* (1969) 4617.
- [53] O. Kratky and G. Porod, *Rec. Trav. Chim.* 68 (1949) 1106.
- [54] L.D. Landau and E.M. Lifshitz, *Statistical physics, course of theoretical physics*, Vol. 5 (Pergamon Press, London, 1958).
- [55] F.H.C. Crick and A. Klug, *Nature* 255 (1975) 530.
- [56] H.M. Sobell, C.C. Tsai, S.C. Jain and S.G. Gilbert, *J. Mol. Biol.* 114 (1977) 333.
- [57] N. Dattagupta, M. Hogan and D.M. Crothers, *Proc. Natl. Acad. Sci. USA* 75 (1978) 4286.
- [58] C.C. Tsai, S.C. Jain and H.M. Sobell, *J. Mol. Biol.* 114 (1977) 301.
- [59] S.C. Jain, C.C. Tsai and H.M. Sobell, *J. Mol. Biol.* 114 (1977) 317.
- [60] T.D. Sakore, S.C. Jain, C.C. Tsai, H.M. Sobell, *Proc. Natl. Acad. Sci. USA* 74 (1977) 188.
- [61] D.M. Crothers, *Biopolymers* 6 (1968) 575.
- [62] J.M. McGhee and P.H. von Hippel, *J. Mol. Biol.* 86 (1974) 469.
- [63] P. Flory, *Statistical mechanics of chain molecules* (Interscience Publ., New York, 1969).
- [64] T.M. Birshtein and O.B. Ptitsyn, *Conformation of macromolecules* (Interscience, New York, 1966).
- [65] W. Müller and D.M. Crothers, *J. Mol. Biol.* 35 (1968) 251.
- [66] K.E. Reinert and H. Thrum, *Studia Biophysica* 24/25 (1970) 319.
- [67] K.E. Reinert, unpublished results.
- [68] R.D. Wells, T.C. Goodman, W. Hillen, G.T. Horn, R.D. Klein, J.E. Larson, U.R. Müller, S.K. Neuendorf, N. Panayotatos and S.M. Stirdivant, *DNA structure and gene regulation in: Progress in nucleic acids research and molecular biology*, Vol. 23, ed. W.E. Cohen.